RESEARCH ARTICLE

Local adaptation in populations of *Mycobacterium tuberculosis* endemic to the Indian Ocean Rim [version 1; peer review: 3 approved]

Fabrizio Menardo[1,2], Liliana K. Rutaihwa[1,2], Michaela Zwyer[1,2], Sonia Borrell[1,2], Iñaki Comas[3], Emilyn Costa Conceição[4,5], Mireia Coscolla[6], Helen Cox[7], Moses Joloba[8], Horng-Yunn Dou[9], Julia Feldmann[1,2], Lukas Fenner[1,2,10], Janet Fyfe[11], Qian Gao[12], Darío García de Viedma[13,14], Alberto L. Garcia-Basteiro[15,16], Sebastian M. Gygli[1,2], Jerry Hella[1,2,17], Hellen Hiza[1,2], Levan Jugheli[1,2], Lujeko Kamwela[1,2,17], Midori Kato-Maeda[18], Qingyun Liu[12], Serej D. Ley[1,2,19], Chloe Loiseau[1,2], Surakameth Mahasirimongkol[20,21], Bijaya Malla[1,2], Prasit Palittapongarnpim[20,21], Niaina Rakotosamimanana[22], Voahangy Rasolofo[22], Miriam Reinhard[1,2], Klaus Reither[2,23], Mohamed Sasamalo[1,2,17], Rafael Silva Duarte[4], Christophe Sola[24,25], Philip Suffys[26], Karla Valeria Batista Lima[27,28], Dorothy Yeboah-Manu[29], Christian Beisel[30], Daniela Brites[1,2], Sebastien Gagneux[1,2]

[1]Department of Medical Parasitology and Infection Biology, Swiss Tropical and Public Health Institute, Basel, Switzerland
[2]University of Basel, Basel, Switzerland
[3]Institute of Biomedicine of Valencia, Valencia, Spain
[4]Instituto de Microbiologia, Federal University of Rio de Janeiro, Rio de Janeiro, Brazil
[5]Instituto Nacional de Infectologia Evandro Chagas, Fundação Oswaldo Cruz, Rio de Janeiro, Brazil
[6]I2SysBio, University of Valencia, Valencia, Spain
[7]Institute of Infectious Diseases and Molecular Medicine, University of Cape Town, Cape Town, South Africa
[8]Department of Medical Microbiology, Makerere University, Kampala, Uganda
[9]National Institute of Infectious Diseases and Vaccinology, National Health Research Institute, Zhunan, Taiwan
[10]Institute for Social and Preventive Medicine, University of Bern, Bern, Switzerland
[11]Victorian Infectious Diseases Reference Laboratory, Melbourne, Australia
[12]Institute of Medical Microbiology, School of Basic Medical Science of Fudan University, Shanghai, China
[13]Instituto de Investigación Sanitaria Gregorio Marañón, Madrid, Spain
[14]CIBER Enfermedades Respiratorias, Madrid, Spain
[15]Barcelona Institute for Global Health, Barcelona, Spain
[16]Centro de Investigação em Saúde de Manhiça, Maputo, Mozambique
[17]Ifakara Health Institute, Bagamoyo, Tanzania
[18]School of Medicine, University of California, San Francisco, USA
[19]Papua New Guinea Institute of Medical Research, Goroka, Papua New Guinea
[20]Department of Microbiology, Mahidol University, Bangkok, Thailand
[21]National Science and Technology Development Agency, Bangkok, Thailand
[22]Institut Pasteur de Madagascar, Antananarivo, Madagascar
[23]Department of Medicine, Swiss Tropical and Public Health Institute, Basel, Switzerland
[24]Université Paris-Saclay, Paris, France
[25]Paris Diderot University, Paris, France
[26]Laboratório de Biologia Molecular Aplicada a Micobactérias, Fundação Oswaldo Cruz, Rio de Janeiro, Brazil

[27]Centro de Ciências Biológicas e da Saúde, Universidade do Estado do Pará, Belém, Brazil
[28]Instituto Evandro Chagas, Ananindeua, Brazil
[29]Noguchi Memorial Institute for Medical Research, University of Ghana, Accra, Ghana
[30]Department of Biosystems Science and Engineering, ETH Zürich, Basel, Switzerland

v1 **First published:** 01 Feb 2021, **10**:60
https://doi.org/10.12688/f1000research.28318.1
Latest published: 01 Feb 2021, **10**:60
https://doi.org/10.12688/f1000research.28318.1

Abstract

Background: Lineage 1 (L1) and 3 (L3) are two lineages of the *Mycobacterium tuberculosis* complex (MTBC) causing tuberculosis (TB) in humans. L1 and L3 are prevalent around the rim of the Indian Ocean, the region that accounts for most of the world's new TB cases. Despite their relevance for this region, L1 and L3 remain understudied.
Methods: We analyzed 2,938 L1 and 2,030 L3 whole genome sequences originating from 69 countries. We reconstructed the evolutionary history of these two lineages and identified genes under positive selection.
Results: We found a strongly asymmetric pattern of migration from South Asia toward neighboring regions, highlighting the historical role of South Asia in the dispersion of L1 and L3. Moreover, we found that several genes were under positive selection, including genes involved in virulence and resistance to antibiotics . For L1 we identified signatures of local adaptation at the *esxH* locus, a gene coding for a secreted effector that targets the human endosomal sorting complex, and is included in several vaccine candidates.
Conclusions: Our study highlights the importance of genetic diversity in the MTBC, and sheds new light on two of the most important MTBC lineages affecting humans.

Keywords

Mycobacterium tuberculosis, adaptation, coevolution

Open Peer Review

Reviewer Status ✓ ✓ ✓

	Invited Reviewers		
	1	**2**	**3**
version 1 01 Feb 2021	✓ report	✓ report	✓ report

1. **Tanvi Honap**, University of Oklahoma, Norman, USA
2. **Miguel Viveiros**, NOVA University Lisbon, Lisbon, Portugal
   João Perdigão, University of Lisbon, Lisbon, Portugal
3. **Ola B. Brynildsrud**, Norwegian Institute of Public Health, Oslo, Norway

Any reports and responses or comments on the article can be found at the end of the article.

Corresponding authors: Fabrizio Menardo (fabrizio.menardo@swisstph.ch), Sebastien Gagneux (sebastien.gagneux@swisstph.ch)

Author roles: Menardo F: Conceptualization, Data Curation, Formal Analysis, Investigation, Methodology, Software, Visualization, Writing – Original Draft Preparation, Writing – Review & Editing; **Rutaihwa LK**: Data Curation, Investigation, Writing – Review & Editing; **Zwyer M**: Data Curation, Writing – Review & Editing; **Borrell S**: Resources, Supervision, Writing – Review & Editing; **Comas I**: Resources, Writing – Review & Editing; **Conceição EC**: Resources; **Coscolla M**: Data Curation; **Cox H**: Resources, Writing – Review & Editing; **Joloba M** : Resources; **Dou HY**: Resources; **Feldmann J**: Investigation; **Fenner L**: Resources; **Fyfe J**: Resources, Writing – Review & Editing; **Gao Q**: Data Curation; **García de Viedma D**: Resources, Writing – Review & Editing; **Garcia-Basteiro AL**: Resources, Writing – Review & Editing; **Gygli SM**: Data Curation, Writing – Review & Editing; **Hella J**: Resources; **Hiza H**: Resources; **Jugheli L**: Resources; **Kamwela L**: Resources; **Kato-Maeda M**: Resources; **Liu Q**: Resources; **Ley SD**: Resources, Writing – Review & Editing; **Loiseau C**: Data Curation, Software; **Mahasirimongkol S**: Resources; **Malla B**: Resources; **Palittapongarnpim P**: Resources, Writing – Review & Editing; **Rakotosamimanana N**: Resources; **Rasolofo V**: Resources; **Reinhard M**: Investigation; **Reither K**: Resources; **Sasamalo M**: Resources; **Silva Duarte R**: Supervision, Writing – Review & Editing; **Sola C**: Resources, Writing – Review & Editing; **Suffys P**: Resources; **Batista Lima KV**: Resources; **Yeboah-Manu D**: Resources; **Beisel C**: Resources, Supervision, Writing – Review & Editing; **Brites D**: Data Curation, Writing – Review & Editing; **Gagneux S**: Conceptualization, Funding Acquisition, Project Administration, Supervision, Writing – Review & Editing

Competing interests: No competing interests were disclosed.

Grant information: This work was supported by the Swiss National Science Foundation (grants 310030_188888, CRSII5_177163, IZRJZ3_164171 and IZLSZ3_170834) and the European Research Council (309540 EVODRTB and 883582-ECOEVODRTB).
The funders had no role in study design, data collection and analysis, decision to publish, or preparation of the manuscript.

How to cite this article: Menardo F, Rutaihwa LK, Zwyer M *et al.* **Local adaptation in populations of *Mycobacterium tuberculosis* endemic to the Indian Ocean Rim [version 1; peer review: 3 approved]** F1000Research 2021, **10**:60 https://doi.org/10.12688/f1000research.28318.1

First published: 01 Feb 2021, **10**:60 https://doi.org/10.12688/f1000research.28318.1

Introduction

The global tuberculosis (TB) epidemic is a major public health emergency, disproportionately affecting vulnerable populations and worsening existing inequalities. Although the estimated incidence and the number of fatalities have slowly decreased over time, every year ten million people develop the disease, and 1.4 million TB patients die (WHO, 2020). Moreover, the Covid-19 pandemic will likely set back the progress toward TB eradication for several years (Glaziou, 2020; Hogan *et al.*, 2020; McQuaid *et al.*, 2020; Saunders & Evans, 2020). TB is spread worldwide, but not all regions are equally affected: 95% of new TB cases occur in Africa and Asia, and the eight countries with the largest burden account for two thirds of the total number of cases (WHO, 2020).

Human TB is caused by members of the *Mycobacterium tuberculosis* complex (MTBC), which includes nine phylogenetic lineages with different geographic distributions. Five of these lineages are restricted to Africa (L5, L6, L7, L8, and L9), while the remaining four (L1, L2, L3, L4) are more broadly distributed (Chihota *et al.*, 2018; Coscollá *et al.*, 2020; Gagneux, 2018; Ngabonziza *et al.*, 2020). While L2 and L4 strains occur across the world, L1 strains are predominantly found around the rim of the Indian Ocean (East Africa, South Asia, and Southeast Asia). L3 has a distinct geographic range (East Africa, Central Asia, Western Asia, and South Asia) that overlaps partially with L1 (Couvin *et al.*, 2019; Wiens *et al.*, 2018). While many MTBC lineages also occur in Northern Europe, North America, Australia and New Zealand, in these low-burden regions, the majority of TB cases are imported through recent migrations, and local transmission is rare (White *et al.*, 2017).

Beyond their geographic distribution, MTBC lineages also differ in virulence, transmissibility, association with drug resistance, and the host immune responses they elicit (Peters *et al.*, 2020). There is an increasing notion that MTBC genetic variation should be considered in the development of new antibiotics and vaccines, and when studying the epidemiology and pathogenesis of the disease (Gagneux, 2017; Peters *et al.*, 2020; Wiens *et al.*, 2018). Yet, much of TB research to date has focused on the laboratory strain H37Rv (belonging to L4) and a few other strains belonging to L2 and L4, because of their broad geographic range, and their association with drug resistance. By contrast, L1 and L3 have largely been neglected, and only few studies have investigated the global populations of these two lineages (Couvin *et al.*, 2019; O'Neill *et al.*, 2019). This knowledge gap is particularly severe as L1 and L3 are endemic to some of the world regions with the heaviest TB burden. For example, L1 and L3 cause the majority of TB cases in India, the country with the highest number of new TB cases in the world, and L1 is by far the most important cause of TB in the Philippines, the country with the 4th highest global TB burden (Wiens *et al.*, 2018). The aim of this study was to characterize the global population structure of L1 and L3 using large-scale population genomics, and to investigate the evolutionary history and selective forces acting on these two lineages.

Results

We screened a large collection of publicly available MTBC genome sequences and selected those belonging to L1 and L3. Additionally, we newly sequenced 767 strains to cover regions that were not well represented in the public data. We applied a series of bioinformatic filters to exclude low quality sequences and mixed infections (Methods), and obtained a curated genome dataset of 4,968 strains (2,938 L1, 2,030 L3). While the phylogenetic tree of L3 showed a ladder-like topology without an evident division in sublineages, L1 comprised five clearly distinct sublineages coalescing close to the root of the tree (*Extended data:* Figures 1 and 2).

The genome sequences included in our final dataset represented 69 countries and covered the known geographic range of L1 and L3 (Methods; *Extended data:* Table 1 and Figures 3 and 4). Because we were interested in studying L1 and L3 in their endemic range, we excluded strains originating from North America, Europe, and Australia from the biogeographic analysis, as in these low-burden regions, most TB patients are recent migrants who were infected in their country of origin (White *et al.*, 2017). We assigned strains to different geographic regions following a modified version of the United Nation geographic scheme (Methods, Figure 1 and Figure 2). Mapping the regions of origin onto the phylogenetic trees revealed that two sublineages of L1 are found almost exclusively in Southeast Asia (L1.1.1 and L1.2.1), while the others are spread over the complete geographic range of L1 (Figure 1; *Extended Data:* Figures 5–6).

We performed a phylogeographic analysis using two alternative approaches (Mascot and PASTML), which are based on different models and inference methods (Ishikawa *et al.*, 2019; Müller *et al.*, 2018). We found that South Asia was predicted to be the geographic range of the Most Recent Common Ancestor (MRCA) of both L1 and L3 (*Extended Data:* Information). Most interestingly, we found a strongly asymmetric pattern of migration. For L1, PASTML identified most migration events from South Asia toward other regions, followed by further dispersion, but almost no back migration to South Asia (Figure 1; *Extended data:* Figure 7 and Files 1 and 2). When we estimated the migration rates with Mascot, we found that the forward migration rate from South Asia toward the rest of the world were 3 to 17 times larger than the migration rates in the opposite direction, confirming the results of PASTML (Figure 1; *Extended data*: Table 2). We found a similar scenario for L3: PASTML inferred the largest number of migrations from South Asia toward East Africa, further spread from East Africa toward neighboring regions, but essentially no migration back to South Asia (Figure 2; *Extended data:* Files 3–4). The Mascot analysis showed that the forward migration rates from South Asia toward East Africa were 26 times larger than the migration rates in the opposite direction (Figure 2; *Extended data:* Table 2).

We performed tip dating to estimate the age of the trees but got inconsistent results for L1, due to a lack of a reliable

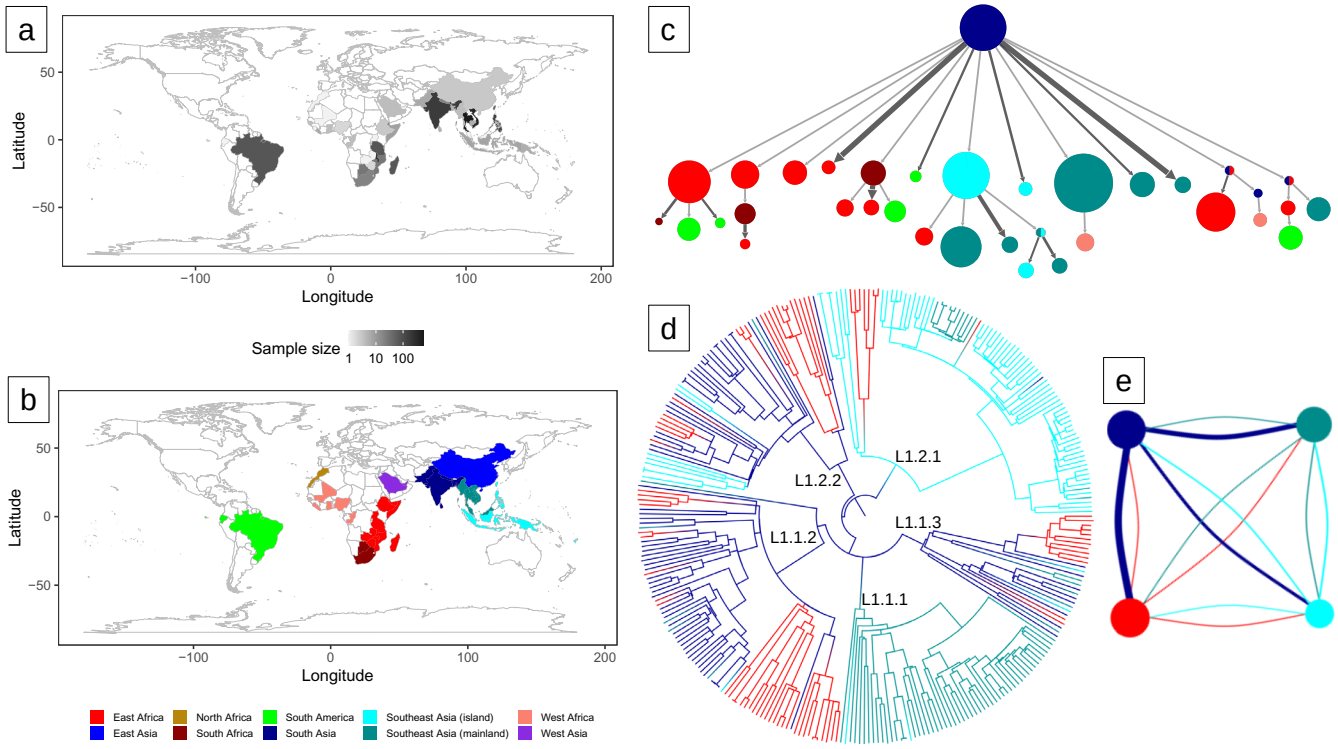

Figure 1. Results of the biogeography analysis: L1. a) Heatmap indicating the origin of the 2,061 L1 strains included in the dataset used for the biogeography analysis. **b)** The geographic regions used in the biogeography analysis of L1. **c)** Results of PASTML (compressed tree), the color code follows the legend of panel (b), the size of the circles is proportional to the number of tips, and the size of the arrows is proportional to the number of times the pattern of migration was observed on the tree. This plot excluded nodes that represented less than three strains. The same plot including all nodes can be found as Extended Data File 1. **d)** Tree obtained with the Mascot analysis; the branches are colored following the legend in panel (b) and represent the inferred ancestral region with the largest posterior probability. **e)** Representation of the relative effective population sizes (circles) and migration rates (lines connecting circles) estimated by Mascot. Lines representing migration rates are colored based on the region of origin (interpreted forward in time). For example, the dark blue line connecting the dark blue circle with the red circle represents the forward migration rate between South Asia and East Africa, which is the largest migration rate estimated by Mascot. The parameter estimates are reported in Extended Data Table 2.

temporal signal (*Extended data:* Information, Figures 8 and 9, Tables 3 and 4). However, the results of a previous study suggested a relatively fast evolutionary rate for L1 (~ 1.4×10^{-7} nucleotide changes per site per year; Menardo *et al.*, 2019), and that the MRCA of L1 lived around the 12th century AD (*Extended data:* Information). By contrast, L3 had a good temporal signal, and different methods estimated that its MRCA lived between the 2nd and the 13th century AD. However, the uncertainty around all of these estimates was very large (*Extended data:* Information, Figure 8, Tables 5 and 6). Together, these results corroborate the findings of previous studies (Bos *et al.*, 2014; Duchêne *et al.*, 2016; Menardo *et al.*, 2019). Calibrating MTBC trees that are hundreds or thousands of years old, with sequences sampled in the last few decades is notoriously challenging and subject to limitations (Menardo *et al.*, 2019). Therefore, we refrain from any strong interpretation of the results of the molecular clock analyses of L1 and L3. We emphasize that the ages reported here are the most likely estimates supported by the available data. Additional data, or alternative methods, might result in different temporal scenarios.

With respect to the geographical aspects, we identified several interesting instances of long-range dispersal. First, we found a clade of L1, composed of 11 strains sampled in five different West African countries. This was surprising because West Africa is usually not considered part of the geographic range of L1. This clade is nested within sublineage L1.1.1, which is essentially only found in mainland Southeast Asia, and the PASTML analysis inferred a direct introduction from Southeast Asia to West Africa. This introduction is unlikely to have happened before the 16th century, when the Portuguese established the maritime route between Europe and Asia by circumnavigating Africa. Assuming that this migration did not occur before the 16th century, we benchmarked the molecular clock of L1 and found that this scenario is indeed compatible with a clock rate equal to, or larger than 1.4×10^{-7} nucleotide changes per site per year, but not with lower ones (*Extended data:* Information, Figure 10).

Second, we found that L1 was introduced to South America on at least 11 independent occasions (Figure 1; *Extended data:*

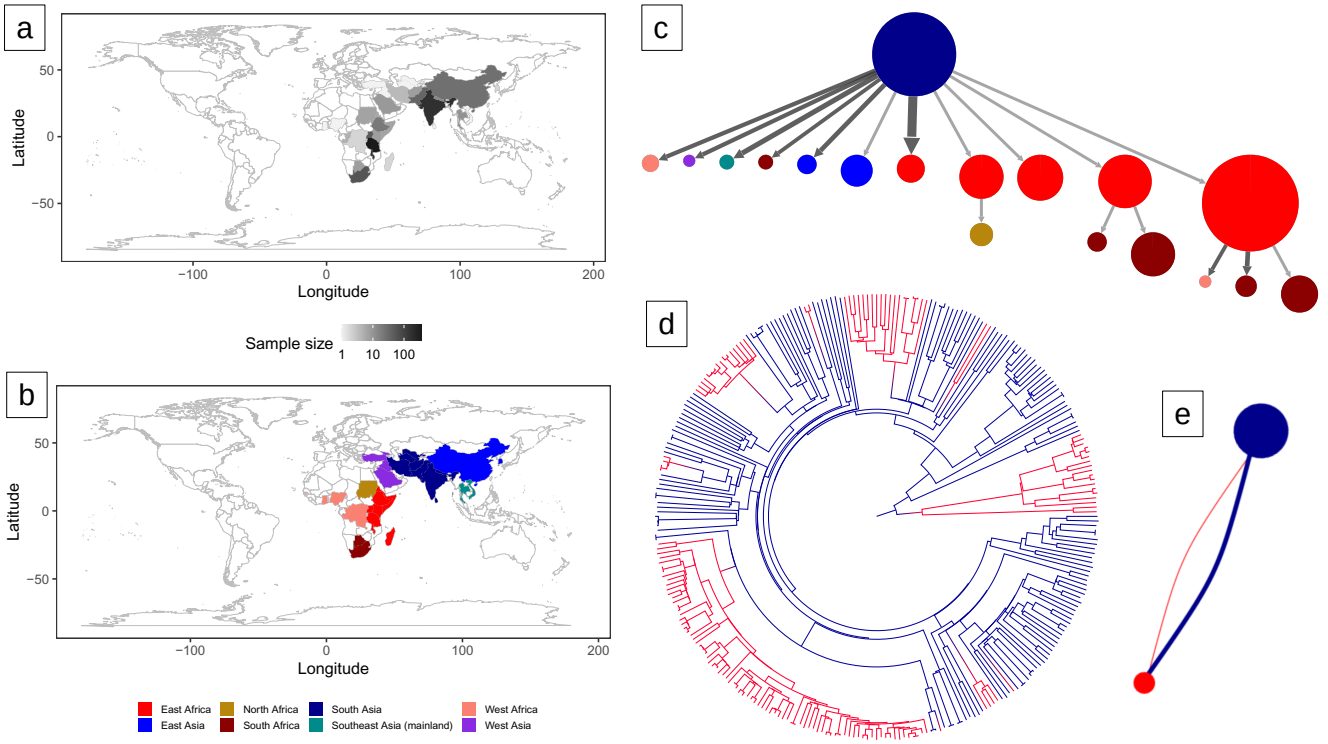

Figure 2. Results of the biogeography analysis: L3. a) Heatmap indicating the origin of 1,021 L3 strains included in the dataset used for the biogeography analysis. **b)** The geographic regions used in the biogeography analysis of L3. **c)** Results of PASTML (compressed tree), the color code follows the legend of panel (**b**), the size of the circles is proportional to the number of tips, and the size of the arrows is proportional to the number of times the pattern of migration was observed on the tree. This plot excluded nodes that represent less than three strains, the same plot including all nodes can be found as Extended Data File 3. **d)** Tree obtained with the Mascot analysis; the branches are colored following the legend in panel (**b**) and represent the inferred ancestral region with the largest posterior probability. **e)** Representation of the relative effective population sizes (circles) and migration rates (lines connecting circles) estimated by Mascot. Lines representing migration rates are colored based on the region of origin (interpreted forward in time). The effective population size of South Asia was estimated to be much larger than the one of East Africa. Additionally, the forward migration rate between South Asia and East Africa was much larger than the one in the opposite direction. The parameter estimates are reported in Extended Data Table 2.

Files 1 and 2). Assuming a clock rate of 1.4×10^{-7}, the earliest introduction was between 1620 and 1830 AD from East Africa, while subsequent introductions occurred from East Africa, South Africa, and South Asia. These results support the hypothesis that L1 was first introduced to Brazil through the slave trade from East Africa (Allen, 2013; Conceição *et al.*, 2019). Interestingly, this is in contrast with L5 and L6, which are endemic to West Africa, but did not establish themselves firmly in South America (De Jong *et al.*, 2010; Rabahi *et al.*, 2020).

Third, similar to the West African clade of L1.1.1, we found an East African clade embedded within sublineage L1.2.1, which otherwise is found almost exclusively in Southeast Asia. This East African clade is composed of 11 strains from five countries, and its sister clade is found in East Timor and Papua New Guinea. We inferred a direct migration from the islands of Southeast Asia to East Africa that occurred between the 13th and the 16th century AD (assuming a clock rate of 1.4×10^{-7}). This would be compatible with early Portuguese expeditions, which reached East Timor and Papua New Guinea in the early 16th century. An alternative explanation could be the Austronesian expansion. Austronesians are thought to have reached the Comoros islands and Madagascar between the 9th and the 13th century AD, possibly through direct navigation from Southeast Asian islands. Malagasy speak an Austronesian language, and Austronesian genetic signatures are found in human populations in the Comoros, Madagascar, and to a small extent also in the Horn of Africa (Blench, 2010; Boivin *et al.*, 2013; Brucato *et al.*, 2016; Brucato *et al.*, 2018; Brucato *et al.*, 2019; Pierron *et al.*, 2014).

L1 and L3 coexist in many regions around the Indian Ocean. Yet, in their evolutionary history, these lineages colonized areas occupied by different human populations. Human genetic variation has been shown to influence the susceptibility to TB (Qu *et al.*, 2011). Most notably, HLA genes play a crucial role in the activation of the immune responses to the MTBC by exposing bacterial peptides (epitopes) to the surface of an infected cell, where they can be recognized by T cells. HLA genes are extremely polymorphic in human populations, and

several alleles of different HLA genes are associated with TB susceptibility in different populations (Brahmajothi *et al.*, 1991; Salie *et al.*, 2014; Sveinbjornsson *et al.*, 2016; Vejbaesya *et al.*, 2002; Yuliwulandari *et al.*, 2010).

Previous studies have shown that T cell epitopes are hyper-conserved in the MTBC, suggesting that immune escape does not provide an advantage and that, contrary to other pathogens, the MTBC needs to be recognized by the immune system and to cause disease in order to transmit (Comas *et al.*, 2010; Coscolla *et al.*, 2015). Our large dataset of L1 and L3 genome sequences from different geographic regions provided an opportunity to scan for lineage- and/or region-specific signatures of selection at T cell epitopes in L1 and L3.

We reconstructed the mutational history of T cell epitopes in L1 and L3, and found that 51% of all epitopes were variable (at the amino acid level) in at least one L1 strain, while only 20% were variable in at least one L3 strain (*Extended data:* Table 7). However, this difference can be explained by the different size and diversity of the two datasets (2,061 genome sequences with 136,023 variable sites for L1; 1,021 genome sequences with 36,316 variable sites for L3). The epitope that accumulated most mutations was located at the N terminus of *esxH* (*Rv0288*). This peptide is a T cell epitope for both classes, MHCI and MHCII; it is also a B cell epitope and was previously identified as one of the few T cell epitopes that were not hyper-conserved (Comas *et al.*, 2010). We found 15 derived haplotypes (at the amino acid level), generated by 28 independent replacements at five positions in a peptide of seven amino acids (Figure 3). By contrast, the second most variable epitope accumulated only seven amino acid changes (*Extended data*: Table 7). Interestingly, we did not find this signature in L3, as all strains carried the ancestral haplotype at the N-terminal *esxH* epitope. Moreover, when we extended the analysis to two large genomic datasets of L2 and L4 strains, we found a much weaker signal: while 21% of L1 strains carried a derived haplotype for this epitope, only 1% of L2 and L4 strains, and no L3 strain had a derived haplotype. Despite analyzing datasets with more strains (6,752 and 10,466 for L2 and L4, respectively), and more polymorphic positions (140,309 and 277,648) compared to L1, we found only three amino acid replacements at the N-terminal epitope of *esxH* in L2, and seven in L4 (Figure 3). The most frequently mutated position was the tenth

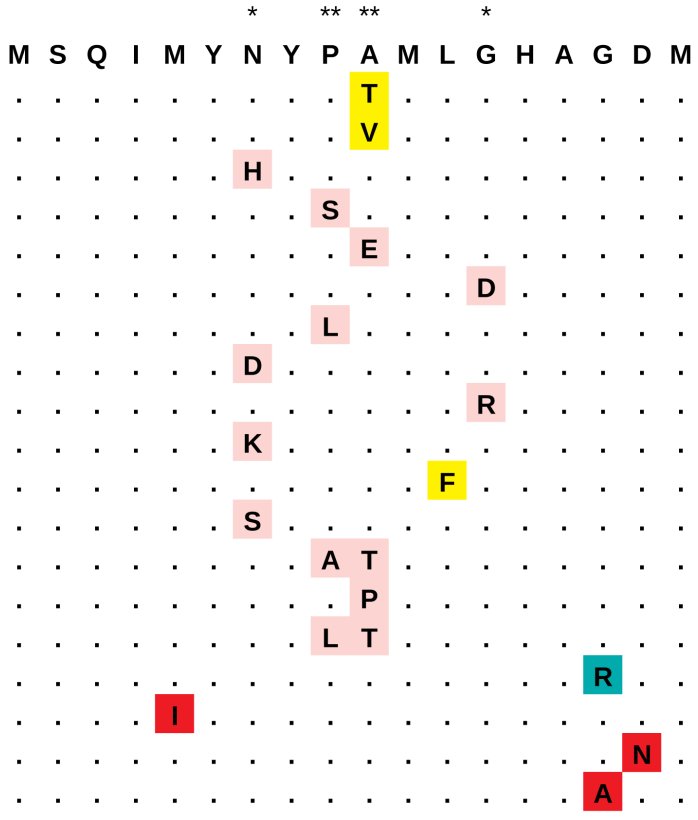

L1	L2	L3	L4
1630	6686	1020	10353
293 (1)	1 (1)	0	0
36 (8)	11 (1)	0	13 (2)
27 (1)	0	0	0
15 (3)	0	0	0
14 (2)	0	0	0
11 (1)	0	0	0
11 (3)	0	0	0
6 (2)	0	0	0
4 (1)	0	0	0
4 (1)	0	0	0
3 (2)	0	0	87 (1)
2 (1)	0	0	0
2 (1)	0	0	0
1 (1)	0	0	0
1 (1)	0	0	0
0	51 (1)	0	0
0	0	0	3 (2)
0	0	0	1 (1)
0	0	0	1 (1)

Figure 3. The hypervariable epitope at the N terminus of *esxH* (aa 1–18). The ancestral epitope is reported in top position, the derived haplotypes are reported below: mutations that were present in more than one lineage are highlighted in yellow, haplotypes that were found exclusively in L1, L2 or L4 are highlighted in pink, blue and red, respectively. Asterisks indicate the position inferred to be under positive selection by PAML: * posterior probability > 0.95: ** posterior probability > 0.99. The table on the right reports for each lineage the number of strains harboring the corresponding haplotype, and between parentheses, the number of independent parallel occurrences of the mutations as inferred by PAUP.

amino acid, where we found 12 independent replacements in L1, and two in L2 and L4 (Figure 3). The amino acid replacement A10V occurred eight times in parallel in L1, once in L2 and twice in L4. The most abundant derived haplotype was caused by a different amino acid replacement at position ten (A10T), which occurred once in L1 and once in L2 (Figure 3). Overall, the replacements in all lineages occurred in eight residues in a peptide of 13 amino acids (Figure 3).

We evaluated the robustness of these results by formally testing for positive selection on the complete sequence of *esxH* using PAML (Yang, 2007). We found that *esxH* was indeed under positive selection in L1 (p-value = 0.00004) but not in the other lineages (p-values = 0.39, 1.00 and 0.65 for L2, L3 and L4, respectively). PAML identified four codons that have been under positive selection in L1 (posterior probability > 0.95), all of them within the N-terminal epitope (codons 7, 9, 10 and 13; Figure 3). Codon 76, which is part of a different T cell epitope, had a posterior probability > 0.9, mutated three times in parallel and was possibly also under positive selection.

Our results further revealed that the derived haplotypes of the N-terminal *esxH* epitope were not distributed randomly across the geographic range of L1. Twenty-two of the 28 (79%) amino acid replacements occurred in sublineages L1.1.1 and L1.2.1, which are almost exclusively present in Southeast Asia (*Extended data:* Figure 11). We constructed a statistical test of association similar to phyC (Farhat *et al.*, 2013) to determine whether replacements in the hypervariable *esxH* epitope were significantly associated with a particular geographic region (Methods). We found that South African strains were less likely to harbor a derived haplotype in the N-terminal *esxH* epitope than expected by chance (empirical p-value = 0.013; Table 1). While East African L1 strains were not associated with the derived haplotypes (empirical p-value = 0.276), we noticed important differences between countries: of the 29 East African strains harboring a derived haplotype, 28 were sampled in Madagascar. When we excluded Madagascar, we found that East Africa had a strong negative association with the derived haplotypes (i.e. East African strains harbored less derived haplotypes than expected by chance; empirical p-value = 0.0004). We then tested the most frequently replaced position (position ten) alone, and again found that East African strains were negatively associated with the derived haplotypes, with and without excluding Malagasy strains (empirical p-values = 0.0176 and 0.034, respectively). Finally, we tested the derived haplotype caused by the most frequent amino acid replacement (A10V; 8 parallel occurrences). Again, we found a negative association with East African strains (empirical p-values = 0.046 and 0.079, respectively including and excluding Malagasy strains; Table 1).

We hypothesized that the accumulation of missense mutations at the N-terminal epitope of *esxH* was due to immune escape. Therefore, we performed *in silico* prediction of the binding affinity of the ancestral haplotype and of the two most frequent

Table 1. Results of the test of association between haplotypes of the N-terminal *esxH* epitope and the geographic region of origin.

Region[1]	Strains[2]	Association[3]	*esxH* (A10V)[4]		*esxH* (A10X)[5]		*esxH* (N terminus)[6]	
			Strains	p-value	Strains	p-value	Strains	p-value
South Asia	219	+	1	0.4852	6	0.385	17	0.453
Southeast Asia (islands)	235	+	10	0.154	156	**0.081**	171	0.174
Southeast Asia (mainland)	982	+	25	0.200	183	**0.095**	210	0.196
East Africa	466	-	0	**0.046**	1	**0.034**	29	0.276
East Africa (no Madagascar)	391	-	0	**0.070**	0	**0.018**	1	**0.0004**
South Africa	49	-	0	0.305	0	0.165	0	**0.013**
South America	77	-	0	0.496	0	0.352	0	**0.095**

[1] We included only regions for which the sample size was 25 or more.

[2] Total number of L1 strains from each region.

[3] All p-values are one-tailed empirical p-values. This column indicates the direction of the association: + we tested for positive association between the derived haplotype(s) and the geographic region; - we tested for negative association between derived haplotype(s) and the geographic region.

[4] Number of strains with the derived haplotype caused by the replacement A10V, and results of the test of association. P-values < than 0.1 are shown in bold.

[5] Number of strains with the derived haplotypes caused by any replacement at position 10 (A10X), and results of the test of association. P-values < than 0.1 are shown in bold.

[6] Number of strains with the derived haplotypes caused by any mutations occurred in the first 18 amino acids of EsxH, and results of the test of association. P-values < than 0.1 are shown in bold.

derived haplotypes (caused by the amino acid replacements A10V and A10T) with different HLA-A, HLA-B and HLA-DRB1 alleles (Methods). We performed this analysis for:

1) Alleles found at high frequency (> 10%) in South- and Southeast Asia, but not in East Africa.

2) Alleles found at high frequency (> 10%) in East Africa, but not in South- and Southeast Asia.

3) Alleles found at high frequency (> 10%) in both regions.

However, we found no differences in the predicted binding affinities between alleles with different geographic distributions (*Extended data:* Table 8).

While *esxH* was the most striking example of a selective pressure specific for one lineage, our analysis suggests that it was not an isolated case. We performed a genome-wide scan for selection with PAML, and identified 17 genes under positive selection, of which five in common between L1 and L3 (*Extended data:* Table 9). We found two genes coding for transmembrane proteins, members of the Esx-1 secretion system, which were under positive selection in L1 (*eccB1* and *eccCa1*, Bonferroni corrected p-values = 0.02 and 0.03), and several genes involved in antibiotic resistance that were under positive selection in both lineages (*Extended data:* Information). We further characterized the profile of drug resistance mutations of L1 and L3, and found that L1 strains harbored a greater proportion of *inhA* promoter mutations (conferring resistance to isoniazid) compared to L3 strains, confirming previous findings (Fenner *et al.*, 2012; *Extended data:* Information, Figure 12, Table 10).

Discussion

Our results highlight the central role of South Asia in the dispersion of L1 and L3. First, we confirmed that the two lineages probably expanded from South Asia (O'Neill *et al.*, 2019). Second, contrary to previous studies that assumed symmetric migration rates between regions (O'Neill *et al.*, 2019), we found that these migrations occurred mostly in one direction. South Asia was a source of migrant strains that fueled the epidemics in other regions, especially in East Africa. Historically, a network of maritime trade, which followed the seasonality of the Monsoons, connected East Africa and South Asia. It is unclear how this could have promoted the spread of TB in one direction, but not in the other. A possible explanation is that strains originating in South Asia were more efficient in transmitting in East Africa, compared to East African strains that migrated to South Asia.

Another difference compared to previous studies is the temporal framework for the evolutionary history of L1. O'Neill *et al.* (2019) estimated that the MRCA of L1 lived in the 4th century BC and that the migration rates decreased after the 7th century AD. Our results indicate that the MRCA of L1 did not exist before the 12th century AD. This discrepancy is due to different assumptions about the clock rates of L1, but none of the two hypotheses can be excluded with the available data. Nonetheless, our discovery of a West African clade that originated through a direct introduction from Southeast Asia supports a faster clock rate of L1, and therefore a more recent MRCA (*Extended data*: Information). As we already mentioned, tip-dating analyses of MTBC trees with roots that are several hundreds of years old is extremely challenging, and the results of such analyses should be taken with caution (Menardo *et al.*, 2019). Moreover, all MTBC molecular clock studies so far assumed that evolutionary rate estimates do not depend on the age of the calibration points (Ho *et al.*, 2005). There are some indications that the effect of time dependency in MTBC datasets is negligible (Pepperell *et al.*, 2013; Menardo *et al.*, 2019). However, this assumption has not yet been thoroughly tested due to the lack of appropriate samples.

We found evidence for a strong selective pressure acting on the N terminus of *esxH* in L1. In contrast, this selective pressure seems to be much reduced, if not absent, in the "modern" lineages (L2, L3 and L4). It is known that L1 strains interact differently with the infected hosts compared to other lineages. For example, L1 strains show a lower virulence in animal models (Bottai *et al.*, 2020), transmit less efficiently in some clinical settings, and infect older patients (Holt *et al.*, 2018). It has been shown recently that the increased virulence of the so-called "modern" MTBC strains is due to the loss of the genomic region TbD1, which remains present in L1 (Bottai *et al.*, 2020). However, it was also reported that in some populations, L1 was associated with higher patient mortality (Smittipat *et al.*, 2019). Given these differences with the "modern" lineages, it is likely that L1 is subject to different selective pressures, and it is possible that the greater selective pressure on *esxH* was caused by some epistatic effect specific to L1.

The signatures of selection at the N-terminal epitope of *esxH* were associated with strains sampled in South- and Southeast Asia, and were almost completely absent in East Africa (excluding Madagascar). Region-specific signatures of positive selection are a hallmark of local adaptation; in this case, adaptation of L1 strains to human hosts with South- and Southeast Asian genotypes. This corroborates previous studies reporting that in Taiwan, L1 is associated with indigenous populations with Austronesian ancestry (reviewed in Dou *et al.*, 2015). This hypothesis is also supported by the L1 population in Madagascar. Madagascar is geographically linked to East Africa, however, Malagasies are genetically distinct from Africans, as they have mixed African and Southeast Asian ancestry due to the Austronesian colonization of Madagascar (Brucato *et al.*, 2016). Madagascar was the region with the second highest prevalence of derived haplotypes in the N-terminal epitope of *esxH* after Southeast Asia (islands), 37.3% and 72.8% respectively, opposed to 0.3% (one single strain) in the rest of East Africa.

Although all the codons under positive selection in *esxH* were contained in one single T cell epitope, the selective pressure acting on *esxH* could be due to some other factor, and not to the binding of the epitope by the MHC, or to its recognition by T cells. A possible mechanism was suggested by experiments

in a mouse model, showing that the N-terminal epitope of EsxH generates an immunodominant CD8 T cells response. The amino acid replacement A10T (which we found to be the most prevalent among the derived haplotypes of the N-terminal EsxH epitope) did not change MHC binding or T cell recognition, but it accelerated the degradation of the epitope, disrupting the immunodominant response (Sutiwisesak *et al.*, 2020; Woodworth *et al.*, 2008).

An additional driver of selection could be the effector function of EsxH. EsxH is a small effector secreted by the Esx-3 secretion system as dimer with EsxG (Ilghari *et al.*, 2011). Within the host macrophages, the dimer EsxH-EsxG targets Hrs (a component of the human endosomal sorting complex), impairing trafficking, and hindering phagosomal maturation and antigen presentation, thus contributing to the survival of the pathogen (Mehra *et al.*, 2013; Mittal *et al.*, 2018; Portal-Celhay *et al.*, 2016). The observed signatures of selection could be due to the adaptation of L1 strains to human genotypes of *hrs* prevalent in South- and Southeast Asia. A similar signature of selection was observed in another Esx effector (EsxW), in MTBC strains belonging to L2 (Holt *et al.*, 2018). Holt and colleagues found evidence for parallel evolution at one residue in the N-terminal loop of EsxW, outside the region covered by known epitopes, suggesting that the selective pressure on EsxW was not due to antigen recognition.

The sampling effort in this study was considerable, and it provided a more complete picture compared to previous studies. Nevertheless, the sampling was not population-based, and for some regions the coverage was scarce (e.g. the Arabian Peninsula). Because of these limitations, our biogeographical analyses were limited to the subcontinental level. This approach revealed the global population structure and the main macroscopic patterns of diversity and migration of L1 and L3. However, MTBC populations are diverse also within subcontinental regions. For example, the MTBC population in Southern India is dominated by L1, while the most prevalent lineage in the North is L3 (Couvin *et al.*, 2019). To investigate fine-scale processes in greater detail, including local adaptation, large population-based studies will be necessary.

In conclusion, the results presented here improve our knowledge about the TB epidemic around the Indian Ocean. A better understanding of the evolutionary dynamics of different MTBC populations might inform the development of control strategies for different regions. For example, *esxH* is part of several new vaccine candidates (Abel *et al.*, 2010; Hoang *et al.*, 2013; Radošević *et al.*, 2007), and at least one of these, H4:IC31, is under clinical development in South Africa (Bekker *et al.*, 2020; Nemes *et al.*, 2018). In the light of our findings, and to develop a globally effective vaccine, it would be important to know if the results of the clinical trials in South Africa can be replicated in Southeast Asia, where there is a high prevalence of derived *esxH* haplotypes in the circulating MTBC populations.

Methods

Strain cultures, DNA extraction and genome sequencing

MTBC isolates previously identified as L1 and L3, either by SNP-typing or spoligotyping, were grown in Middlebrook 7H9 liquid medium supplemented with ADC and incubated at 37°C. Purified genomic DNA was obtained from cultures using a CTAB extraction method. Whole genome sequencing was performed on libraries prepared from purified genomic DNA using Illumina Nextera ® XT library and NEBNext ® Ultra TM II FS DNA Library Prep Kits. Sequencing was performed using the Illumina HiSeq 2500 or NextSeq 500 paired-end technology.

The sequence data generated by this study has been deposited on SRA under the accession numbers PRJNA630228 and PRJNA670836.

Bioinformatic pipeline

We screened a large collection of publicly available whole genome sequences (Illumina) of MTBC strains belonging to L1 and L3, using the diagnostic SNPs described in Steiner *et al.* (2014). To cover geographic regions that were under-represented by this dataset, we additionally sequenced the genomes of 767 clinical strains (360 L1, and 407 L3).

For all samples, Illumina reads were trimmed with Trimmomatic v0.33 (SLIDINGWINDOW: 5:20,ILLUMINACLIP:{adapter}:2:30:10) (Bolger *et al.*, 2014). Reads shorter than 20 bp were excluded from the downstream analysis. Overlapping paired-end reads were then merged with SeqPrep (overlap size = 15; https://github.com/jstjohn/SeqPrep). The resulting reads were mapped to the reconstructed MTBC ancestral sequence (Comas *et al.*, 2013) with BWA v0.7.12 (mem algorithm; Li & Durbin, 2010). Duplicated reads were marked by the MarkDuplicates module of Picard v 2.1.1 (https://github.com/broadinstitute/picard). The RealignerTargetCreator and IndelRealigner modules of GATK v.3.4.0 (McKenna *et al.*, 2010) were used to perform local realignment of reads around Indels. Reads with alignment score lower than (0.93*read_length)-(read_length*4*0.07)) were excluded: this corresponds to more than 7 miss-matches per 100 bp.

SNPs were called with Samtools v1.2 mpileup (Li *et al.*, 2009) and VarScan v2.4.1 (Koboldt *et al.*, 2012) using the following thresholds: minimum mapping quality of 20, minimum base quality at a position of 20, minimum read depth at a position of 7X, minimum percentage of reads supporting the call 90%. SNPs in previously defined repetitive regions were excluded (i.e. PPE and PE-PGRS genes, phages, insertion sequences and repeats longer than 50 bp) as described before (Brites *et al.*, 2018).

We applied the following filters: genomes were excluded if they had 1) an average coverage <15x, 2) more than 50% of their SNPs excluded due to the strand bias filter, 3) more than

50% (or more than 1,000 in absolute number) of their SNPs having a percentage of reads supporting the call between 10% and 90%, 4) contained single nucleotide polymorphisms diagnostic for different MTBC lineages (Steiner *et al.*, 2014), as this indicated that a mix of genomes was sequenced, 5) had more than 5,000 SNPs of difference compared to the reconstructed ancestral genome of the MTBC (Comas *et al.*, 2013). Additionally, when multiple strains were sampled from the same patient, we retained only one. We further excluded all strains that had less SNPs than (average - (3 * standard deviation)) of the respective lineage (calculated after all previous filtering steps). We built SNP alignments for L1 and L3 separately, including only variable positions with less than 10% of missing data, and finally, we excluded all genomes with more than 10% of missing data in the alignment of the respective lineage. After all filtering steps, we were able to retrieve 4,968 strains with high quality genome sequences for further analyses (2,938 L1, 2,030 L3; *Extended data:* Table 1).

Analysis of sublineages

We used the curated datasets and inferred phylogenetic trees based on all polymorphic positions (excluding the ones in repetitive regions, see above) with raxml 8.2.11 (Stamatakis, 2014; -m GTRCAT and -V options). We then identified sublineages following the classification (and using the diagnostic SNPs) of Coll *et al.* (2014).

Molecular clock analyses with LSD

We selected all strains for which the year of sampling was known (2,499 strains, 1,672 L1, 827 L3). For both lineages, we built SNP alignments including only variable positions with less than 10% of missing data. We inferred phylogenetic trees with RAxML 8.2.11 (Stamatakis, 2014), using the GTR model (-m GTRCAT -V options). Since the alignments contain only variable positions, we rescaled the branch lengths of the trees: rescaled_branch_length = ((branch_length * alignment_lengths) / (alignment_length + invariant_sites)). We rooted the trees using the genome sequence of a L2 strain as outgroup (accession number SAMEA4441446).

We used the least square method implemented in LSD v0.3-beta (To *et al.*, 2016) to estimate the molecular clock rate with the QPD algorithm and calculating the confidence interval (options -f 100 and -s). We also performed a date randomization test by randomly reassigning the sampling dates among taxa 100 times and estimating the clock rate from the randomized and observed datasets. All LSD analyses were performed on the two lineages individually (L1 and L3), and on the five sublineages of L1.

Molecular clock analyses with Beast

Bayesian molecular clock analyses are computationally demanding and they would be impossible to apply onto the complete datasets. Therefore, we sub-sampled the L1 and L3 datasets used for the LSD analysis to 400 genomes with two different strategies: 1) random subsampling 2) random subsampling keeping at least 25 genomes for each year of sampling (where possible; "weighted subsampling"). For this second subsampling strategy, we used Treemmer v0.3 (Menardo *et al.*, 2018) with options -X 400, -pr, -lm, and -mc 25. For both subsampling schemes, we generated three subsets of the original datasets, resulting in six subsets for each lineage. We assembled SNP alignments including only variable positions with less than 10% of missing data, and used jModelTest 2.1.10 v20160303 (Darriba *et al.*, 2012) to identify the best fitting nucleotide substitution model (according to the Akaike information criterion) among 11 possible schemes including unequal nucleotide frequencies (total models = 22, options -s 11 and -f).

We performed Bayesian inference with Beast 2.5 (Bouckaert *et al.*, 2019). We corrected the xml files to specify the number of invariant sites as indicated here: https://groups.google.com/forum/#!topic/beast-users/QfBHMOqImFE, and used the tip sampling year as calibration. We assumed the best fitting nucleotide substitution model as identified by jModelTest, a relaxed lognormal clock model (Drummond *et al.*, 2006) and an exponential population size coalescent prior. We chose a 1/x prior for the population size [0–109], a 1/x prior for the mean of the lognormal distribution of the clock rate [10−10−10−5], a normal(0,1) prior for the standard deviation of the lognormal distribution of the clock rate [0 –infinity]. For the exponential growth rate prior, we used the standard Laplace distribution [-infinity–infinity]. For all datasets, we ran at least two runs, we used Tracer 1.7.1 (Rambaut *et al.*, 2018) to identify and exclude the burn-in, to evaluate convergence among runs and to calculate the estimated sample size. We stopped the runs when at least two chains reached convergence, and the ESS of the posterior and of all parameters were larger than 200.

Since we detected a strong temporal signal only for L3, we performed a set of additional analyses of the subsets of L3. We repeated the Beast analysis with an extended Bayesian Skyline Plot (BSP) prior instead of the exponential growth prior, and performed a nested sampling analysis (Russel *et al.*, 2019) to identify which of these two models (exponential growth and extended BSP) fitted the data best. The nested sampling was run with chainLength = 20000, particleCount= 4, and subChainLength = 10000.

All xml input files are available as Supplementary Files in *Extended data.*

Datasets for biogeography analyses

For the biogeography analysis, we considered only genome sequences obtained from strains for which the locality of sampling was known. When the country of sampling did not correspond to the country of origin of the patient (or was unknown), we considered as sampling locality the country of origin of the patient (this affected 187 strains, 121 L1 and 66 L3). Furthermore, similarly to other studies (O'Neill *et al.*, 2019), we excluded all genomes that were sampled from Europe, North America and Australia, as most contemporary infections in these regions affect recent migrants. The final dataset for the biogeography analyses comprised 3,082 strains (2,061 L1 and 1,021 L3). We assigned the different isolates to different

subcontinental geographic regions according to sampling locality. To do this, we followed a modified version of the United Nations geographic scheme (https://unstats.un.org/unsd/methodology/m49/; *Extended data:* Table 1 and Figures 1–3).

Phylogeography analysis with PASTML

For both lineages, we built SNP alignments including only variable positions with less than 10% of missing data, and all strains with known sampling locality (excluding strains from North America, Europe and Australia; see above, 2,061 L1 genomes and 1,021 L3 genomes). We inferred phylogenetic trees with raxml 8.2.11 (Stamatakis, 2014), using the GTR model (-m GTRCAT -V options). Since the alignments contain only variable positions, we re-scaled the branch lengths of the trees: rescaled_branch_length = ((branch_length * alignment_lengths) / (alignment_length + invariant_sites)).

Since PASTML needs a time tree as input, we calibrated the phylogenies with LSD, assuming a clock rate of 1.4×10^{-7} for L1, and 9×10^{-8} for L3. In this analysis, genomes for which the sampling date was not known were assumed to have been sampled between 1995 and 2018, which is the period in which all strains with known date of isolation were sampled. Importantly, using different clock rates for this analysis would only change the time scale of the trees, but not the reconstruction of the ancestral characters.

We assigned to each strain the subcontinental geographic region of origin as character, and used PASTML (Ishikawa *et al.*, 2019) to reconstruct the ancestral geographical ranges and their changes along the trees of L1 and L3. We used the MPPA as prediction method (standard settings) and added the character predicted by the joint reconstruction even if it was not selected by the Brier score (option -forced_joint). Additionally, we repeated the PASTML analysis for the sublineages of L1 individually.

Phylogeography analysis with Mascot

As a complementary method to reconstruct the ancestral range and the migration pattern of different populations, we used the Beast package Mascot (Müller *et al.*, 2018). We assumed that strains sampled in the different subcontinental regions represent distinct subpopulations, and we considered only populations for which we had at least 75 genome sequences: four populations for L1 (East Africa, South Asia, Southeast Asia (mainland) and Southeast Asia (islands)), and two populations for L3 (East Africa and South Asia). For computational reasons, we subsampled the two datasets (L1 and L3) to ~300 strains. We sampled an equal number of strains from each geographic region (where possible), and within regions, we randomly sampled an equal number of strains from each country (where possible). This sub-sampling scheme resulted in two subsets of 303 and 300 strains for L1 and L3, respectively.

We assembled SNP alignments including only variable positions with less than 10% of missing data, and used jModelTest 2.1.10 v20160303 (Darriba *et al.*, 2012) to identify the best fitting nucleotide substitution model as described above.

We performed Bayesian inference with Beast2.5 (Bouckaert *et al.*, 2019). We corrected the xml files to specify the number of invariant sites as indicated here: https://groups.google.com/forum/#!topic/beast-users/QfBHMOqImFE. We assumed a lognormal uncorrelated clock and we fixed the mean of the lognormal distribution of the clock rate to 1.4×10^{-7} (L1) and 9×10^{-8} (L3). We assigned the tip sampling years to the different strains, and when the sampling time was unknown, we assumed a uniform prior from 1995 to 2018 (similarly to what done in the PASTML analysis). We further assumed the best fitting nucleotide substitution model as identified by jModelTest, a gamma prior for the standard deviation of the lognormal distribution of the clock rate [0 –infinity], and a lognormal prior for the population size with standard deviation = 0.2, and mean estimated in real space. Finally, we used an exponential distribution with mean = 10^{-4} as prior for the migration rates. For each analysis, we ran at least two runs. We used Tracer 1.7.1 (Rambaut *et al.*, 2018) to identify and exclude the burn-in, to evaluate convergence among runs, and to calculate the estimated sample size. We stopped the runs when at least two chains reached convergence, and the ESS of the posterior, prior and of the parameters of interest (population sizes and migration rates) were larger than 200.

The xml input files are available as Supplementary Files in *Extended data.*

L2 and L4 datasets

For the analysis of *esxH*, we wanted to compare the results obtained for L1 and L3 with the other two major human-adapted MTBC lineages L2 and L4. Therefore, we compiled two datasets of publicly available genome sequences for these two lineages. We applied the same bioinformatic pipeline described above: genomes were excluded if they had 1) an average coverage <15x, 2) more than 50% (or more than 1,000 in absolute number) of their SNPs having a percentage of reads supporting the call between 10% and 90%, or 3) contained single nucleotide polymorphisms diagnostic for different MTBC lineages (Steiner *et al.*, 2014), as this could indicate mixed infection. The final dataset consisted of 6,752 L2 genome sequences (with 140,309 polymorphic positions) and 10,466 L4 genome sequences (with 277,648 polymorphic positions; *Extended data:* Table 1). We reconstructed the phylogenetic tree of L2 with raxml 8.2.11 (Stamatakis, 2014) as described above. Due to the large size of the dataset, we used FastTree (Price *et al.*, 2010) with options -nt -nocat -nosupport to reconstruct the phylogenetic tree of L4.

Epitopes analysis

We downloaded the amino acid sequence of all MTBC epitopes described for *Homo sapiens* from the immune epitope database (https://www.iedb.org/; downloaded on the 03.08.2020). We considered separately MHCI epitopes and MHCII epitopes. We mapped the epitope sequences onto the H37Rv genome (GCF_000195955.2) using tblastn and excluded sequences mapping equally well to multiple loci in the H37Rv genome. Additionally, we retained only epitopes that mapped with two mismatches or less over the whole epitope length. This

resulted in a final list of 539 MHCI epitopes, and 1,144 MHCII epitopes. (*Extended data:* Table 7). We used the datasets obtained for the biogeography analysis (2,061 genome sequences for L1, and 1,021 genome sequences for L3).

For each lineage, we independently assembled a multiple sequence alignment for each epitope. We then translated the sequence to amino acids and used PAUP 4.a (Wilgenbusch & Swofford, 2003) to reconstruct the replacement history of all polymorphic positions on the rooted phylogenetic trees. We used two maximum parsimony algorithms (ACCTRAN and DELTRAN) and considered only the events reconstructed by both algorithms.

Analysis of esxH

We considered the first 18 amino acids of *esxH* (MSQIMYNYPAMLGHAGDM), which was by far the epitope with most amino acid replacements in L1. We expanded the analysis of this epitope to the L2 and L4 datasets, so that we could compare the results with L1 and L3. For the PAML analysis, we randomly selected 500 strains from each MTBC lineage. We used the phylogenetic tree reconstructed by RAxML (same settings as above), and the gene alignment to estimate the branch lengths of the tree using the M0 codon model implemented in PAML 4.9e (Yang, 2007). This step was necessary to obtain a tree with the branch length in expected substitutions per codon. We then fitted two alternative codon models (M1a and M2a) to the trees and alignments. M1a allows ω to be variable across sites, and it assumes two different ω ($0 < \omega_0 < 1$, and $\omega_1 = 1$), modeling nearly neutral evolution; M2a assumes one additional ω ($\omega_2 > 1$) compared to M1a, thus modeling positive selection. We performed a likelihood ratio test between the two models as described in Zhang *et al.* (2005). Templates for the control files of the codeml analyses (M0, M1a, M2a) are available as Supplementary Files in *Extended data*. The codon under positive selection were identified with the Bayes empirical Bayes method (Yang *et al.*, 2005).

To test whether the derived haplotypes of this epitope were associated with a specific geographic region, we constructed a statistical test analogous to PhyC (Farhat *et al.*, 2013), which is normally used to test for association between a variant and phenotypic drug resistance. We simulated mutations on the phylogenetic tree of L1 and counted how many strains from each region resulted to have a derived state according to the simulation. Under this procedure, mutations occur randomly on the tree, and therefore independently from the geographic region where the tips were sampled. For each test, we performed 10,000 simulations to obtain a null distribution, and we compared this distribution to the observed data to obtain empirical p-values. We used the same geographic region used for the biogeography analysis. Additionally, we considered East Africa excluding Madagascar.

R code and input files to perform this test are available as Supplementary Files in *Extended data*.

Prediction of binding affinity between T cell epitopes and HLA alleles

We considered three HLA loci: HLA-A, HLA-B and HLA-DRB1. We used the allele frequency database (Gonzalez-Galarza *et al.*, 2020) to identify alleles that are prevalent in East Africa and not in South Asia and Southeast Asia, or the other way around. Because the coverage of the allele frequency database is patchy, we focused on the following countries: Kenya and Zimbabwe as representatives of East Africa; India, Thailand and Taiwan as representatives of South- and Southeast Asia. We identified:

1) Alleles that had a frequency of 10% or more in at least one population in South- and Southeast Asia, but had frequencies lower than 10% in all East African populations.

2) Alleles that had a frequency of 10% or more in at least one population in East Africa, but had frequencies lower than 10% in all populations in South- and Southeast Asia.

3) Alleles that had a frequency of 10% or more in at least one population both in South- and Southeast Asia and in East Africa.

For all these alleles, we performed *in silico* binding prediction with three epitopes: the ancestral epitope at the *esxH* N terminus (MSQIMYNYPAMLGHAGDM), and the two most frequently observed derived epitopes (MSQIMYNYPTMLGHAGDM, and MSQIMYNYPVMLGHAGDM). For HLA-A and HLA-B alleles, we used the NetMHCPan4.1 server (Reynisson *et al.*, 2020) with standard settings. For HLA-DRB1 alleles, we used the prediction tool of the immune epitope database (https://www.iedb.org/).

Genome wide scan for positive selection with PAML

For this analysis, we used the subsets generated for the Mascot analysis. These datasets are representative of the populations of L1 and L3 in their core geographic ranges, and are computationally treatable. We generated sequence alignments for all genes individually, excluding genes in repetitive regions of the genome (see above). Because some genes are deleted in L1 but not in L3, or the other way around, we obtained a slightly different number of gene alignments for the two lineages (L1: 3,623, L3: 3,622). For each gene, we performed a test for positive selection with PAML as described above for *esxH*. We considered as under positive selection all genes, for which the likelihood ratio test resulted in a Bonferroni-corrected p-value < 0.05.

Drug resistance mutations profiles

We considered 196 mutations conferring resistance to different antibiotics (Payne *et al.*, 2019). We extracted the respective genomic positions from the vcf file of the 4,968 genomes of the complete curated data set (2,938 L1, 2,030 L3) and assembled them in phylip format. To determine the number of independent

mutations, we reconstructed the nucleotide changes on the phylogenetic tree rooted with the L2 strain (SAMEA4441446). To do this, we used the maximum parsimony ACCTRAN and DELTRAN algorithms implemented in PAUP 4.0a (Wilgenbusch & Swofford, 2003), and considered only the events reconstructed by both algorithms.

Data availability

Underlying data

The sequence data generated by this study has been deposited on SRA (https://www.ncbi.nlm.nih.gov/sra) under the accession numbers PRJNA630228 and PRJNA670836.

Extended data

Extended data is available here: https://github.com/fmenardo/MTBC_L1_L3.

DOI: https://doi.org/10.5281/zenodo.4435760 (Menardo, 2021).

This project contains the following extended data:

- The folder Supplementary_text_figures_tables contains supplementary text, figures and tables.
- Supplementary_file_1.html: PASTML results for L1, compressed tree.
- Supplementary_file_2.html: PASTML results for L1, complete tree.
- Supplementary_file_3.html: PASTML results for L3, compressed tree.
- Supplementary_file_4.html: PASTML results for L3, complete tree.
- The folder Dating_Beast contains the xml files for the dating analyses.
- The folder EsxH_haplotype_association_test contains the code and input files to perfomr the test of association between different haplotypes and geographic regions.
- The folder EsxH_PAML contains the control files and input files to perform the positive selection analysis on EsxH.
- The folder Mascot contains the xml files for the Mascot analyses.

Acknowledgements

Calculations were performed at sciCORE (http://scicore.unibas.ch/) scientific computing core facility at the University of Basel.

References

Abel B, Tameris M, Mansoor N, *et al.*: **The novel tuberculosis vaccine, AERAS-402, induces robust and polyfunctional CD4⁺ and CD8⁺ T cells in adults.** *Am J Respir Crit Care Med.* 2010; **181**(12): 1407–1417.
PubMed Abstract | Publisher Full Text | Free Full Text

Allen RB: **Indian Ocean transoceanic migration, 16th–19th century.** *The Encyclopedia of Global Human Migration.* 2013.
Publisher Full Text

Bekker LG, Dintwe O, Fiore-Gartland A, *et al.*: **A phase 1b randomized study of the safety and immunological responses to vaccination with H4:IC31, H56:IC31, and BCG revaccination in *Mycobacterium tuberculosis*-uninfected adolescents in Cape Town, South Africa.** *EClinicalMedicine.* 2020; **21**: 100313.
PubMed Abstract | Publisher Full Text | Free Full Text

Blench R: **Evidence for the Austronesian voyages in the Indian Ocean.** *The Global Origins and Development of Seafaring.* 2010; **239**: 48.
Reference Source

Boivin N, Crowther A, Helm R, *et al.*: **East Africa and Madagascar in the Indian Ocean world.** *J World Prehist.* 2013; **26**(3): 213–281.
Publisher Full Text

Bolger AM, Lohse M, Usadel B: **Trimmomatic: a flexible trimmer for Illumina sequence data.** *Bioinformatics.* 2014; **30**(15): 2114–2120.
PubMed Abstract | Publisher Full Text | Free Full Text

Bos KI, Harkins KM, Herbig A, *et al.*: **Pre-Columbian mycobacterial genomes reveal seals as a source of New World human tuberculosis.** *Nature.* 2014; **514**(7523): 494–497.
PubMed Abstract | Publisher Full Text | Free Full Text

Bottai D, Frigui W, Sayes F, *et al.*: **TbD1 deletion as a driver of the evolutionary success of modern epidemic *Mycobacterium tuberculosis* lineages.** *Nat Commun.* 2020; **11**(1): 684.
PubMed Abstract | Publisher Full Text | Free Full Text

Bouckaert R, Vaughan TG, Barido-Sottani J, *et al.*: **BEAST 2.5: An advanced software platform for Bayesian evolutionary analysis.** *PLoS Comput Biol.* 2019; **15**(4): e1006650.
PubMed Abstract | Publisher Full Text | Free Full Text

Brahmajothi V, Pitchappan RM, Kakkanaiah VN, *et al.*: **Association of pulmonary tuberculosis and HLA in south India.** *Tubercle.* 1991; **72**(2): 123–132.
PubMed Abstract | Publisher Full Text

Brites D, Loiseau C, Menardo F, *et al.*: **A new phylogenetic framework for the animal-adapted *Mycobacterium tuberculosis* complex.** *Front Microbiol.* 2018; **9**: 2820.
PubMed Abstract | Publisher Full Text | Free Full Text

Brucato N, Fernandes V, Kusuma P, *et al.*: **Evidence of Austronesian Genetic Lineages in East Africa and South Arabia: Complex Dispersal from Madagascar and Southeast Asia.** *Genome Biol Evol.* 2019; **11**(3): 748–758.
PubMed Abstract | Publisher Full Text | Free Full Text

Brucato N, Fernandes V, Mazières S, *et al.*: **The Comoros Show the Earliest Austronesian Gene Flow into the Swahili Corridor.** *Am J Hum Genet.* 2018; **102**(1): 58–68.
PubMed Abstract | Publisher Full Text | Free Full Text

Brucato N, Kusuma P, Cox MP, *et al.*: **Malagasy Genetic Ancestry Comes from an Historical Malay Trading Post in Southeast Borneo.** *Mol Biol Evol.* 2016; **33**(9): 2396–2400.
PubMed Abstract | Publisher Full Text | Free Full Text

Chihota VN, Niehaus A, Streicher EM, *et al.*: **Geospatial distribution of *Mycobacterium tuberculosis* genotypes in Africa.** *PLoS One.* 2018; **13**(8): e0200632.
PubMed Abstract | Publisher Full Text | Free Full Text

Coll F, McNerney R, Guerra-Assuncao JA, *et al.*: **A robust SNP barcode for typing *Mycobacterium tuberculosis* complex strains.** *Nat Commun.* 2014; **5**(1): 4812.
PubMed Abstract | Publisher Full Text | Free Full Text

Comas I, Chakravartti J, Small PM, *et al.*: **Human T cell epitopes of Mycobacterium tuberculosis are evolutionarily hyperconserved.** *Nat Genet.* 2010; **42**(6): 498–503.
PubMed Abstract | Publisher Full Text | Free Full Text

Comas I, Coscolla M, Luo T, *et al.*: **Out-of-Africa migration and Neolithic**

coexpansion of *Mycobacterium tuberculosis* with modern humans. *Nat Genet* 2013; **45**(10): 1176–1182.
PubMed Abstract | Publisher Full Text | Free Full Text

Conceição EC, Refregier G, Gomes HM, *et al.*: ***Mycobacterium tuberculosis* lineage 1 genetic diversity in Pará, Brazil, suggests common ancestry with east-African isolates potentially linked to historical slave trade.** *Infect Genet Evol.* 2019; **73**: 337–341.
PubMed Abstract | Publisher Full Text

Coscollá M, Brites D, Menardo F, *et al.*: **Phylogenomics of *Mycobacterium africanum* reveals a new lineage and a complex evolutionary history.** *bioRxiv.* 2020.
Publisher Full Text

Coscolla M, Copin R, Sutherland J, *et al.*: ***M. tuberculosis* T Cell Epitope Analysis Reveals Paucity of Antigenic Variation and Identifies Rare Variable TB Antigens.** *Cell Host Microbe.* 2015; **18**(5): 538–548.
PubMed Abstract | Publisher Full Text | Free Full Text

Couvin D, Reynaud Y, Rastogi N: **Two tales: Worldwide distribution of Central Asian (CAS) versus ancestral East-African Indian (EAI) lineages of *Mycobacterium tuberculosis* underlines a remarkable cleavage for phylogeographical, epidemiological and demographical characteristics.** *PLoS One.* 2019; **14**(7): e0219706.
PubMed Abstract | Publisher Full Text | Free Full Text

Darriba D, Taboada GL, Doallo R, *et al.*: **jModelTest 2: more models, new heuristics and parallel computing.** *Nat Methods.* 2012; **9**(8): 772.
PubMed Abstract | Publisher Full Text | Free Full Text

De Jong BC, Antonio M, Gagneux S: ***Mycobacterium africanum*--review of an important cause of human tuberculosis in West Africa.** *PLoS Negl Trop Dis.* 2010; **4**(9): e744.
PubMed Abstract | Publisher Full Text | Free Full Text

Dou HY, Chen YY, Kou SC, *et al.*: **Prevalence of *Mycobacterium tuberculosis* strain genotypes in Taiwan reveals a close link to ethnic and population migration.** *J Formos Med Assoc.* 2015; **114**(6): 484–488.
PubMed Abstract | Publisher Full Text

Drummond AJ, Ho SYW, Phillips MJ, *et al.*: **Relaxed phylogenetics and dating with confidence.** *PLoS Biol.* 2006; **4**(5): e88.
PubMed Abstract | Publisher Full Text | Free Full Text

Duchêne S, Holt KE, Weill FX, *et al.*: **Genome-scale rates of evolutionary change in bacteria.** *Microb Genom.* 2016; **2**(11): e000094.
PubMed Abstract | Publisher Full Text | Free Full Text

Farhat MR, Shapiro BJ, Kieser KJ, *et al.*: **Genomic analysis identifies targets of convergent positive selection in drug-resistant *Mycobacterium tuberculosis*.** *Nat Genet.* 2013; **45**(10): 1183–1189.
PubMed Abstract | Publisher Full Text | Free Full Text

Fenner L, Egger M, Bodmer T, *et al.*: **Effect of mutation and genetic background on drug resistance in *Mycobacterium tuberculosis*.** *Antimicrob Agents Chemother.* 2012; **56**(6): 3047–3053.
PubMed Abstract | Publisher Full Text | Free Full Text

Gagneux S (Ed.): **Strain variation in the Mycobacterium tuberculosis complex: its role in biology, Epidemiology and Control.** *Springer.* 2017; **1019**.
Publisher Full Text

Gagneux S: **Ecology and evolution of *Mycobacterium tuberculosis*.** *Nat Rev Microbiol.* 2018; **16**(4): 202–213.
PubMed Abstract | Publisher Full Text

Glaziou P: **Predicted impact of the COVID-19 pandemic on global tuberculosis deaths in 2020.** *medRxiv.* 2020.
Publisher Full Text

Gonzalez-Galarza FF, McCabe A, Santos EJMD, *et al.*: **Allele frequency net database (AFND) 2020 update: gold-standard data classification, open access genotype data and new query tools.** *Nucleic Acids Res.* 2020; **48**(D1): D783–D788.
PubMed Abstract | Publisher Full Text | Free Full Text

Ho SYW, Phillips MJ, Cooper A, *et al.*: **Time dependency of molecular rate estimates and systematic overestimation of recent divergence times.** *Mol Biol Evol.* 2005; **22**(7): 1561–1568.
PubMed Abstract | Publisher Full Text

Hoang T, Aagaard C, Dietrich J, *et al.*: **ESAT-6 (EsxA) and TB10.4 (EsxH) based vaccines for pre- and post-exposure tuberculosis vaccination.** *PLoS One.* 2013; **8**(12): e80579.
PubMed Abstract | Publisher Full Text | Free Full Text

Hogan AB, Jewell BL, Sherrard-Smith E, *et al.*: **Potential impact of the COVID-19 pandemic on HIV, tuberculosis, and malaria in low-income and middle-income countries: a modelling study.** *Lancet Glob Health.* 2020; **8**(9): e1132–e1141.
PubMed Abstract | Publisher Full Text | Free Full Text

Holt KE, McAdam P, Thai PVK, *et al.*: **Frequent transmission of the *Mycobacterium tuberculosis* Beijing lineage and positive selection for the EsxW Beijing variant in Vietnam.** *Nat Genet.* 2018; **50**(6): 849–856.
PubMed Abstract | Publisher Full Text | Free Full Text

Ilghari D, Lightbody KL, Veverka V, *et al.*: **Solution Structure of the *Mycobacterium tuberculosis* EsxG·EsxH Complex functional implications and comparisons with other m. tuberculosis esx family complexes.** *J Biol Chem.* 2011; **286**(34): 29993–30002.
PubMed Abstract | Publisher Full Text | Free Full Text

Ishikawa SA, Zhukova A, Iwasaki W, *et al.*: **A fast likelihood method to reconstruct and visualize ancestral scenarios.** *Mol Biol Evol.* 2019; **36**(9): 2069–2085.
PubMed Abstract | Publisher Full Text | Free Full Text

Koboldt DC, Zhang Q, Larson DE, *et al.*: **VarScan 2: somatic mutation and copy number alteration discovery in cancer by exome sequencing.** *Genome Res.* 2012; **22**(3): 568–576.
PubMed Abstract | Publisher Full Text | Free Full Text

Li H, Durbin R: **Fast and accurate long-read alignment with Burrows-Wheeler transform.** *Bioinformatics.* 2010; **26**(5): 589–595.
PubMed Abstract | Publisher Full Text | Free Full Text

Li H, Handsaker B, Wysoker A, *et al.*: **The sequence alignment/map format and SAMtools.** *Bioinformatics.* 2009; **25**(16): 2078–2079.
PubMed Abstract | Publisher Full Text | Free Full Text

McKenna A, Hanna M, Banks E, *et al.*: **The Genome Analysis Toolkit: a MapReduce framework for analyzing next-generation DNA sequencing data.** *Genome Res.* 2010; **20**(9): 1297–1303.
PubMed Abstract | Publisher Full Text | Free Full Text

McQuaid CF, McCreesh N, Read JM, *et al.*: **The potential impact of COVID-19-related disruption on tuberculosis burden.** *Eur Respir J.* 2020; **56**(2): 2001718.
PubMed Abstract | Publisher Full Text | Free Full Text

Mehra A, Zahra A, Thompson V, *et al.*: ***Mycobacterium tuberculosis* type VII secreted effector EsxH targets host ESCRT to impair trafficking.** *PLoS Pathog.* 2013; **9**(10): e1003734.
PubMed Abstract | Publisher Full Text | Free Full Text

Menardo F: **fmenardo/MTBC_L1_L3: MTBC L1 L3 (Version v2).** *Zenodo.* 2021.
http://www.doi.org/10.5281/zenodo.4435760

Menardo F, Duchêne S, Brites D, *et al.*: **The molecular clock of *Mycobacterium tuberculosis*.** *PLoS Pathog.* 2019; **15**(9): e1008067.
PubMed Abstract | Publisher Full Text | Free Full Text

Menardo F, Loiseau C, Brites D, *et al.*: **Treemmer: a tool to reduce large phylogenetic datasets with minimal loss of diversity.** *BMC Bioinformatics.* 2018; **19**(1): 164.
PubMed Abstract | Publisher Full Text | Free Full Text

Mittal E, Skowyra ML, Uwase G, *et al.*: ***Mycobacterium tuberculosis* type VII secretion system effectors differentially impact the ESCRT endomembrane damage response.** *mBio.* 2018; **9**(6): e01765–18.
PubMed Abstract | Publisher Full Text | Free Full Text

Müller NF, Rasmussen D, Stadler T: **MASCOT: parameter and state inference under the marginal structured coalescent approximation.** *Bioinformatics.* 2018; **34**(22): 3843–3848.
PubMed Abstract | Publisher Full Text | Free Full Text

Nemes E, Geldenhuys H, Rozot V, *et al.*: **Prevention of *M. tuberculosis* infection with H4:IC31 vaccine or BCG revaccination.** *N Engl J Med.* 2018; **379**(2): 138–149.
PubMed Abstract | Publisher Full Text | Free Full Text

Ngabonziza JCS, Loiseau C, Marceau M, *et al.*: **A sister lineage of the *Mycobacterium tuberculosis* complex discovered in the African Great Lakes region.** *Nat Commun.* 2020; **11**(1): 2917.
PubMed Abstract | Publisher Full Text | Free Full Text

O'Neill MB, Shockey A, Zarley A, *et al.*: **Lineage specific histories of *Mycobacterium tuberculosis* dispersal in Africa and Eurasia.** *Mol Ecol.* 2019; **28**(13): 3241–3256.
PubMed Abstract | Publisher Full Text | Free Full Text

Qu HQ, Fisher-Hoch SP, McCormick JB: **Knowledge gaining by human genetic studies on tuberculosis susceptibility.** *J Hum Genet.* 2011; **56**(3): 177–182.
PubMed Abstract | Publisher Full Text | Free Full Text

Payne JL, Menardo F, Trauner A, *et al.*: **Transition bias influences the evolution of antibiotic resistance in *Mycobacterium tuberculosis*.** *PLoS Biol.* 2019; **17**(5): e3000265.
PubMed Abstract | Publisher Full Text | Free Full Text

Pepperell CS, Casto AM, Kitchen A, *et al.*: **The role of selection in shaping diversity of natural *M. tuberculosis* populations.** *PLoS Pathog.* 2013; **9**(8): e1003543.
PubMed Abstract | Publisher Full Text | Free Full Text

Peters JS, Ismail N, Dippenaar A, *et al.*: **Genetic Diversity in *Mycobacterium tuberculosis* Clinical Isolates and Resulting Outcomes of Tuberculosis Infection and Disease.** *Annu Rev Genet.* 2020; **54**: 511–537.
PubMed Abstract | Publisher Full Text

Pierron D, Razafindrazaka H, Pagani L, *et al.*: **Genome-wide evidence of Austronesian-Bantu admixture and cultural reversion in a hunter-gatherer group of Madagascar.** *Proc Natl Acad Sci U S A.* 2014; **111**(3): 936–941.
PubMed Abstract | Publisher Full Text | Free Full Text

Portal-Celhay C, Tufariello JM, Srivastava S, *et al.*: ***Mycobacterium tuberculosis* EsxH inhibits ESCRT-dependent CD4 $^+$ T-cell activation.** *Nat Microbiol.* 2016; **2**(2): 16232.
PubMed Abstract | Publisher Full Text | Free Full Text

Price MN, Dehal PS, Arkin AP: **FastTree 2--approximately maximum-likelihood trees for large alignments.** *PLoS One.* 2010; **5**(3): e9490.
PubMed Abstract | Publisher Full Text | Free Full Text

Rabahi MF, Conceição EC, de Paiva LO, *et al.*: **Characterization of *Mycobacterium tuberculosis* var. *africanum* isolated from a patient with**

pulmonary tuberculosis in Brazil. *Infect Genet Evol.* 2020; **85**: 104550.
PubMed Abstract | Publisher Full Text

Radošević K, Wieland CW, Rodriguez A, *et al.*: **Protective immune responses to a recombinant adenovirus type 35 tuberculosis vaccine in two mouse strains: CD4 and CD8 T-cell epitope mapping and role of gamma interferon.** *Infect Immun.* 2007; **75**(8): 4105–4115.
PubMed Abstract | Publisher Full Text | Free Full Text

Rambaut A, Drummond AJ, Xie D, *et al.*: **Posterior summarization in Bayesian phylogenetics using Tracer 1.7.** *Syst Biol.* 2018; **67**(5): 901–904.
PubMed Abstract | Publisher Full Text | Free Full Text

Reynisson B, Alvarez B, Paul S, *et al.*: **NetMHCpan-4.1 and NetMHCIIpan-4.0: improved predictions of MHC antigen presentation by concurrent motif deconvolution and integration of MS MHC eluted ligand data.** *Nucleic Acids Res.* 2020; **48**(W1): W449–W454.
PubMed Abstract | Publisher Full Text | Free Full Text

Russel PM, Brewer BJ, Klaere S, *et al.*: **Model selection and parameter inference in phylogenetics using Nested Sampling.** *Syst Biol.* 2019; **68**(2): 219–233.
PubMed Abstract | Publisher Full Text

Salie M, van der Merwe L, Möller M, *et al.*: **Associations between human leukocyte antigen class I variants and the *Mycobacterium tuberculosis* subtypes causing disease.** *J Infect Dis.* 2014; **209**(2): 216–223.
PubMed Abstract | Publisher Full Text | Free Full Text

Saunders MJ, Evans CA: **COVID-19, tuberculosis and poverty: preventing a perfect storm.** *Eur Respir J.* 2020; **56**(1): 2001348.
PubMed Abstract | Publisher Full Text | Free Full Text

Smittipat N, Miyahara R, Juthayothin T, *et al.*: **Indo-Oceanic *Mycobacterium tuberculosis* strains from Thailand associated with higher mortality.** *Int J Tuberc Lung Dis.* 2019; **23**(9): 972–979.
PubMed Abstract | Publisher Full Text

Stamatakis A: **RAxML version 8: a tool for phylogenetic analysis and post-analysis of large phylogenies.** *Bioinformatics.* 2014; **30**(9): 1312–1313.
PubMed Abstract | Publisher Full Text | Free Full Text

Steiner A, Stucki D, Coscolla M, *et al.*: **KvarQ: targeted and direct variant calling from fastq reads of bacterial genomes.** *BMC Genomics.* 2014; **15**(1): 881.
PubMed Abstract | Publisher Full Text | Free Full Text

Sutiwisesak R, Hicks ND, Boyce S, *et al.*: **A natural polymorphism of *Mycobacterium tuberculosis* in the *esxH* gene disrupts immunodomination by the TB10.4-specific CD8 T cell response.** *PLoS Pathog.* 2020; **16**(10): e1009000.
PubMed Abstract | Publisher Full Text | Free Full Text

Sveinbjornsson G, Gudbjartsson DF, Halldorsson BV, *et al.*: ***HLA* class II sequence variants influence tuberculosis risk in populations of European ancestry.** *Nat Genet.* 2016; **48**(3): 318–322.
PubMed Abstract | Publisher Full Text | Free Full Text

To TH, Jung M, Lycett S, *et al.*: **Fast dating using least-squares criteria and algorithms.** *Syst Biol.* 2016; **65**(1): 82–97.
PubMed Abstract | Publisher Full Text | Free Full Text

Vejbaesya S, Chierakul N, Luangtrakool K, *et al.*: **Associations of HLA class II alleles with pulmonary tuberculosis in Thais.** *Eur J Immunogenet.* 2002; **29**(5): 431–434.
PubMed Abstract | Publisher Full Text

White Z, Painter J, Douglas P, *et al.*: **Immigrant arrival and tuberculosis among large immigrant- and refugee-receiving countries, 2005–2009.** *Tuberc Res Treat.* 2017; **2017**: 8567893.
PubMed Abstract | Publisher Full Text | Free Full Text

Wiens KE, Woyczynski LP, Ledesma JR, *et al.*: **Global variation in bacterial strains that cause tuberculosis disease: a systematic review and meta-analysis.** *BMC Med.* 2018; **16**(1): 196.
PubMed Abstract | Publisher Full Text | Free Full Text

Wilgenbusch JC, Swofford D: **Inferring evolutionary trees with PAUP.** *Curr Protoc Bioinformatics.* 2003; (1): 6–4.
PubMed Abstract | Publisher Full Text

Woodworth JS, Wu Y, Behar SM: **Mycobacterium tuberculosis-specific CD8+ T cells require perforin to kill target cells and provide protection *in vivo*.** *J Immunol.* 2008; **181**(12): 8595–8603.
PubMed Abstract | Publisher Full Text | Free Full Text

World Health Organization: **Global Tuberculosis Report.** 2020.
Reference Source

Yang Z: **PAML 4: phylogenetic analysis by maximum likelihood.** *Mol Biol Evol.* 2007; **24**(8): 1586–1591.
PubMed Abstract | Publisher Full Text

Yang Z, Wong WS, Nielsen R: **Bayes empirical Bayes inference of amino acid sites under positive selection.** *Mol Biol Evol.* 2005; **22**(4): 1107–1118.
PubMed Abstract | Publisher Full Text

Yuliwulandari R, Sachrowardi Q, Nakajima H, *et al.*: **Association of HLA-A, -B, and -DRB1 with pulmonary tuberculosis in western Javanese Indonesia.** *Hum Immunol.* 2010; **71**(7): 697–701.
PubMed Abstract | Publisher Full Text

Zhang J, Nielsen R, Yang Z: **Evaluation of an improved branch-site likelihood method for detecting positive selection at the molecular level.** *Mol Biol Evol.* 2005; **22**(12): 2472–2479.
PubMed Abstract | Publisher Full Text

Open Peer Review

Current Peer Review Status: ✔ ✔ ✔

Version 1

Reviewer Report 15 March 2021

https://doi.org/10.5256/f1000research.31323.r79710

✔ **Ola B. Brynildsrud**
Division of Infectious Disease Control and Environmental Health, Norwegian Institute of Public Health, Oslo, Norway

In the paper "Local adaptation in populations of Mycobacterium tuberculosis endemic to the Indian Ocean Rim", Menardo and colleagues explore diversity, phylogeographic relationships and patterns of adaptation in TB lineages 1 and 3, both of which are distributed mainly around the Indian Ocean. The paper demonstrates a strongly asymmetric trend of South Asian spread to other regions. Further, it describes a search for positive selection throughout these genomes, and identify one gene in particular, exsH, as being a target for T-cell dependent selection. The authors additionally calibrates molecular clocks for both L1 and L3 and use this to date certain events in the tree.

The methodology is solid and well suited to answer the questions posed. I found the paper to be well written and helpful in shedding light on important questions related to the evolution of L1 and L3. I have only a few minor discussion points.

Now, the clock analyses are not heavily emphasized, but I thought it might be a potential flaw that the calibration rests on the assumption that the foundation of a single sub-lineage in West Africa could not have happened prior to the establishment of Portuguese sailing routes around the tip of Africa. While I'm certainly not an expert on historic migrations or anthropology, I would assume there must be many possible alternative scenarios. (For example, pilgrimages across the Sahara are known to have happened much prior to this). As far as I can tell, this calibration is the major driving force for the difference in L1 TMRCA from O'Neill. It would be interesting to know how the degree to which this calibration affects the TMRCA and clock rate. On a somewhat related note, this article fails to cite some key references on the phylogeography of TB.

In one section the authors evaluate association between esxH haplotypes and the geographic region of origin. They calculate this association using a home-made statistical test based on phyC. I could not gather from the description exactly what they measure. It is a simulation-based test that measures "how many strains from each region resulted to have a derived state according to

the simulation". Is there a test statistic being ranked here? Is it single-region vs the rest or is the statistic a composite measure of multiple regions? How is the simulation for the null distribution set up? E.g. is it a forward-in-time simulation using a specified mutation rate or a permutation or something else? I see that the code for running this test is posted on github - However, I still think a few more details in the actual paper is in order for the biologists that don't read R. Speaking of this test, It is a bit unconvential for Table 1 to highlight all results with P<0.1, especially since a large number of associations are being tested here. I would not consider p<0.1 to be particularly strong evidence of association.

I'd like to commend the authors for making so much of their data publicly available. Datasets are in immediately-usable formats which makes it simple to download all the raw data, and as mentioned code is also readily available.

Very minor:

- HLA abbreviation never explained in manuscript.
- Tip date randomisation performed, but the results of this test is never stated.
- Why is PRJNA630228 posted? As far as I can tell it doesnt contain any SRA data, and the other accession contains data for all 767 strains.

Is the work clearly and accurately presented and does it cite the current literature?
Yes

Is the study design appropriate and is the work technically sound?
Yes

Are sufficient details of methods and analysis provided to allow replication by others?
Yes

If applicable, is the statistical analysis and its interpretation appropriate?
Yes

Are all the source data underlying the results available to ensure full reproducibility?
Yes

Are the conclusions drawn adequately supported by the results?
Yes

Competing Interests: No competing interests were disclosed.

Reviewer Expertise: Bioinformatics, microbial genomics

I confirm that I have read this submission and believe that I have an appropriate level of expertise to confirm that it is of an acceptable scientific standard.

Reviewer Report 01 March 2021

https://doi.org/10.5256/f1000research.31323.r79237

Miguel Viveiros
Global Health and Tropical Medicine, GHTM, Institute of Hygiene and Tropical Medicine, IHMT, NOVA University Lisbon, Lisbon, Portugal
João Perdigão
Research Institute for Medicines (iMed.ULisboa), Faculty of Pharmacy, University of Lisbon, Lisbon, Portugal

This study depicts a very interesting and relevant account on the evolutionary history and phylogeography of *Mycobacterium tuberculosis* of Lineages 1 and 3. Historically, and while forming an important part of the *M. tuberculosis* species diversity, the study of both lineages have been neglected in comparison to Lineages 2 and 4. The authors of this study assembled a large genomic dataset encompassing 2938 and 2030 L1 and L3 isolates, respectively, and by implementing distinct molecular evolutionary algorithms were able to put forward a scenario for the dissemination of these strains. A South Asian origin is proposed for both clades from where these strains appeared to have radiated via migration-driven dispersion towards East Africa (L3) and other regions (L1). The weakest aspect of the work is the lack of phylogeographic and historical context of L1 and L3 versus L2 and L4 dissemination, especially L4 in South-America and L2 in Asia in the context of the migratory waves.

The authors used PASTML and Mascot to conduct the phylogeographic analyses, revealing the migratory pattern of these lineages from South Asia revealing the origins of these two lineages. Several genes involved in virulence and drug resistance were shown to be under positive selection in L1 and L3 strains with important adaptative consequences. Importantly, *esxH* derived haplotypes were not randomly distributed through the geographic range of L1 and the finding of positive selection acting on vaccine candidates, such as this, is important and deserves attention.

The manuscript is very well written, easy to read and understand and the methods are robust and well applied and described. Important to note the absence of a few important references to other groups work on the third wave migration of migrations in the 16th century that impacted the dissemination of L1 in Africa and other regions.

Some comments that can be useful for discussion:

The analysis pertaining the introduction of L1 to South America is based on a more modest number of isolates (n=77), all but one from Brazil. This limits the robusteness of the conclusions for this region. It is possible that the evolutionary history of L1 in South America is far more complex than the one outlined in the article and there may be missing links. For example, EAI (L1) strains have been detected in several South and Central American countries (Mexico, Peru,

Panama, Colombia, etc.) and besides slave trade, the Spain-operated Manila-Acapulco Galleon trade route (est. ca. 1568) connected Southeast Asia to Central and South America.

Regarding the L1.1.1 sub-lineage, what precludes these strains to have been introduced to West Africa in a more recent period other than the XVI or the XVII century? As far as we can tell, this pertains a group of 10 isolates scattered over five countries, but what is the degree of divergence between these isolates? Eventually, can this also be linked with the indentured labor promoted by the British Empire in the XIX century?

On the epitope analysis, upon downloading epitopes from IEDB did the authors include only epitopes with positive assays and was there a threshold for including only epitopes validated by independent assays (more reliable)? Also, how did overlapping epitopes been handled?

Is the work clearly and accurately presented and does it cite the current literature?
Yes

Is the study design appropriate and is the work technically sound?
Yes

Are sufficient details of methods and analysis provided to allow replication by others?
Yes

If applicable, is the statistical analysis and its interpretation appropriate?
Yes

Are all the source data underlying the results available to ensure full reproducibility?
Yes

Are the conclusions drawn adequately supported by the results?
Yes

Competing Interests: No competing interests were disclosed.

Reviewer Expertise: Mycobacteriology, Tuberculosis, Laboratory Diagnosis and Molecular Epidemiology.

We confirm that we have read this submission and believe that we have an appropriate level of expertise to confirm that it is of an acceptable scientific standard.

Reviewer Report 17 February 2021

https://doi.org/10.5256/f1000research.31323.r78953

Tanvi Honap
University of Oklahoma, Norman, OK, USA

The aim of this study was to conduct a phylogeographic analysis of *Mycobacterium tuberculosis* complex (MTBC) strains belonging to Lineages 1 and 3, which are the most prevalent lineages in South Asian countries with a high TB burden, such as India. The authors compiled an excellent dataset of nearly 5,000 MTBC genomes from these two lineages, comprising publicly available as well as newly-sequenced MTBC strains. Their phylogenomic analyses showed that L1 comprises a further five distinct sublineages, whereas L3 does not contain distinct sublineages. The authors used two different methods (PASTML and Mascot) for conducting phylogeographic analyses, with results from both methods suggesting an interesting asymmetric pattern of migration: these lineages originated in and migrated from South Asia to other regions, with very little back-migration into South Asia. This underscores the important role South Asia has played in the dispersal of these lineages. The authors found several genes involved in virulence and antibiotic resistance to be under positive selection in L1 and L3 strains. Lastly, the authors also found evidence of local adaptation at the esxH epitope in L1 strains from South and Southeast Asia, which requires further study as this epitope is a part of several vaccine candidates.

Overall, I found this to be a well-designed and thorough study, and a very well-written manuscript. I have no major concerns and only a few minor suggestions for aesthetic improvement:

- The Methods section titled "*Strain cultures, DNA extraction and genome sequencing*" is missing citations for the methods used (eg. CTAB extraction method).
- Figures 1A and 2A heatmaps would look better in color than grayscale.
- The Supplementary Information would benefit from a thorough proofreading for grammatical and typological errors.

Is the work clearly and accurately presented and does it cite the current literature?
Yes

Is the study design appropriate and is the work technically sound?
Yes

Are sufficient details of methods and analysis provided to allow replication by others?
Yes

If applicable, is the statistical analysis and its interpretation appropriate?
Yes

Are all the source data underlying the results available to ensure full reproducibility?
Yes

Are the conclusions drawn adequately supported by the results?
Yes

Competing Interests: No competing interests were disclosed.

Reviewer Expertise: Pathogen genomics

I confirm that I have read this submission and believe that I have an appropriate level of expertise to confirm that it is of an acceptable scientific standard.